Engineered plant control of associative nitrogen fixation

PNAS RESEARCH ARTICLE | MICROBIOLOGY

Engineered plant control of associative nitrogen fixation

Timothy L. Haskett[a,1], Ponraj Paramasivan[b], Marta D. Mendes[a], Patrick Green[a], Barney A. Geddes[a,c], Hayley E. Knights[a], Beatriz Jorrin[a], Min-Hyung Ryu[d], Paul Brett[e], Christopher A. Voigt[d], Giles E. D. Oldroyd[b], and Philip S. Poole[a,1]

Edited by Éva Kondorosi, Hungarian Academy of Sciences, Biological Research Centre, Szeged, Hungary; received September 22, 2021; accepted March 11, 2022

Engineering N_2-fixing symbioses between cereals and diazotrophic bacteria represents a promising strategy to sustainably deliver biologically fixed nitrogen (N) in agriculture. We previously developed novel transkingdom signaling between plants and bacteria, through plant production of the bacterial signal rhizopine, allowing control of bacterial gene expression in association with the plant. Here, we have developed both a homozygous rhizopine producing (*RhiP*) barley line and a hybrid rhizopine uptake system that conveys upon our model bacterium *Azorhizobium caulinodans* ORS571 (*Ac*) 10^3-fold improved sensitivity for rhizopine perception. Using this improved genetic circuitry, we established tight rhizopine-dependent transcriptional control of the nitrogenase master regulator *nifA* and the N metabolism σ-factor *rpoN*, which drove nitrogenase expression and activity in vitro and in situ by bacteria colonizing *RhiP* barley roots. Although in situ nitrogenase activity was suboptimally effective relative to the wild-type strain, activation was specific to *RhiP* barley and was not observed on the roots of wild-type plants. This work represents a key milestone toward the development of a synthetic plant-controlled symbiosis in which the bacteria fix N_2 only when in contact with the desired host plant and are prevented from interaction with nontarget plant species.

rhizopine | nitrogen fixation | rhizobium | barley | symbiosis

Exploitation of symbiotic and associative bacterial N_2 fixation (the reduction of $N_2 \rightarrow NH_3$) represents a key strategy to sustainably meet the rising nitrogen (N)-demands of modern-day agriculture (1). Maintaining productivity of major cereal crops—such as wheat, maize, barley, and rice—which constitute over 50% of global human caloric intake, is paramount (2, 3). In contrast to legumes, cereals lack the genetic components required to establish intimate associations with N_2-fixing rhizobial bacteria, but their root compartments are naturally colonized by associative epiphytic and endophytic diazotrophic bacteria that are estimated to fix up to 5 Tg N ha^{-1} yr^{-1} in global agrosystems (3–6). In some instances, inoculation of cereals with associative diazotrophic bacteria has a positive influence on yield (7, 8), though responses are typically inconsistent largely because of failure of inoculants to competitively colonize root systems and reach quorum density (9). Furthermore, the costly energy demands of N_2 fixation have driven the evolution of multilayered genetic mechanisms in bacteria that repress N_2 fixation and favor NH_3 assimilation over release to plants (10).

Delivery of biologically fixed N could be improved by engineering the N_2-fixing catalyst nitrogenase or the capacity for nodule symbiosis directly into cereals (11–14). Alternatively, preexisting associative bacterial N_2-fixing interactions could be genetically manipulated for improved function (9, 15–17). Overriding negative feedback regulation of N_2 fixation to permit excess production and release of NH_3 to plants represents a focal point for the latter strategy (10, 18). However, a lack of stringent host-specificity for root colonization by the bacteria (6, 9) would allow growth promotion of target and nontarget plants species alike. Establishing host-plant control of engineered bacterial traits would provide specificity to such interactions. Plant–microbe signaling circuitry has already been engineered into tobacco plants, conveying them with the ability to synthesize bacterial acylhomoserine lactones (AHL), which activated gene expression in bacterial AHL biosensors and restored biocontrol activity and pathogenicity of AHL synthase-deficient *Pseudomonas aureofaciens* and *Erwinia carotovora* mutants, respectively (19). Similarly, opine producing *Arabidopsis* plants generated by *Agrobacterium*-mediated transformation were shown to selectively enrich the rhizosphere for opine catabolizing bacteria (20–22), with ratio and population density positively correlating with the input of opines (23). Critically, AHLs exhibit poor signaling specificity (24, 25), whereas opines induce pathogenic agrobacteria to form crown galls on plants (26); therefore, these signaling circuits may be suboptimal for control of N_2-fixation and other plant–microbe interactions in agriculture.

Significance

Inoculation of cereals with diazotrophic (N_2-fixing) bacteria offers a sustainable alternative to the application of nitrogen fertilizers in agriculture. While natural diazotrophs have evolved multilayered regulatory mechanisms that couple N_2 fixation with assimilation of the product NH_3 and prevent release to plants, genetic modifications can permit excess production and excretion of NH_3. However, a lack of stringent host-specificity for root colonization by the bacteria would allow growth promotion of target and nontarget plants species alike. Here, we exploit synthetic transkingdom signaling to establish plant host-specific control of the N_2-fixation catalyst nitrogenase in *Azorhizobium caulinodans* occupying barley roots. This work demonstrates how partner-specific interactions can be established to avoid potential growth promotion of nontarget plants.

Author contributions: T.L.H. and P.S.P. designed research; T.L.H., P.P., M.D.M., P.G., B.A.G., H.E.K., B.J., and P.B. performed research; T.L.H., P.P., P.G., B.A.G., H.E.K., B.J., M.-H.R., C.A.V., and G.E.D.O. contributed new reagents/analytic tools; T.L.H., P.P., M.D.M., P.G., B.A.G., H.E.K., B.J., P.B., and P.S.P. analyzed data; and T.L.H., P.P., C.A.V., G.E.D.O., and P.S.P. wrote the paper.

The authors declare no competing interest.

This article is a PNAS Direct Submission.

[1]To whom correspondence may be addressed. Email: tim.haskett@plants.ox.ac.uk or philip.poole@plants.ox.ac.uk.

This article contains supporting information online at http://www.pnas.org/lookup/suppl/doi:10.1073/pnas.2117465119/-/DCSupplemental.

Published April 11, 2022.

To develop a more practical plant–microbe signaling circuit, we engineered into barley and *Medicago* a synthetic biosynthesis pathway for production of the rhizopine signaling molecule *scyllo*-inosamine (SI), which is exuded from the roots and can be perceived by bacteria carrying a rhizopine receiver plasmid on the root surface and rhizosphere (27, 28). The pathway requires *myo*-inositol as a substrate, which is converted to *scyllo*-inosose by an inositol dehydrogenase (IolG/IdhA) and then to SI by the aminotransferase (MosB), both of which are expressed constitutively in the plant (27). In nature, rhizopines including SI and 3-*O*-methyl *scyllo*-inosamine (3-*O*-MSI) are synthesized by rhizobia occupying nodules under control of the nitrogenase master regulator NifA (28). They are excreted from the nodule and enhance nodulation competitiveness in progeny strains carrying the catabolic *moc* genes, but do not increase the population size of these bacteria occupying the rhizosphere (29). As a signaling molecule, SI exhibits a high degree of specificity, with only a few species of *Rhizobium* and *Sinorhizobium* identified that catabolize it as a nutrient source (28, 30, 31). Furthermore, SI does not stimulate pathogenic behavior by resident bacteria, as is true of opines (32).

Here, we built upon our rhizopine signaling circuitry to establish host-plant control of associative N_2 fixation by the model cereal endophyte *Azorhizobium caulinodans* ORS571 (here termed *Ac*). Previously, we established tight control over free-living N_2 fixation in response to exogenous supplementation of *Ac* cultures with synthetic and plant-derived chemicals (15). This involved replacing the native master regulator of N_2 fixation *nifA* with chemically inducible *nifA* or *nifA-rpoN* controller plasmids driving the expression of the large suite of *nif* and *fix* genes required for assembly and function of nitrogenase. Controlled expression of *nifA* circumvented natural transcriptional repression by N, whereas N-mediated posttranslational repression of NifA was partially overcome by expressing a $NifA_{L94Q/D95Q}$ variant protein that is defective in sensing N status (15). Because mechanisms such as the DraT-DraG system that directly inhibit nitrogenase activity in response to N availability are absent in *Ac* (33–35), regulated $NifA_{L94Q/D95Q}$ expression permits control of N_2 fixation that is partially resistant to feedback inhibition by the product NH_3 (15).

In this study, we develop a homozygous rhizopine-producing (*RhiP*) barley line and bacterial SI receiver plasmid that conveys markedly improved sensitivity to rhizopine perception in *Ac*. With this improved sensitivity, we established tight rhizopine-dependent transcriptional control of *nifA* and a variant gene encoding $NifA_{L94Q/D95Q}$ (15) that when coexpressed with the N metabolism σ-factor, drove partially NH_3-resistant, rhizopine-inducible nitrogenase activity in vitro. We also demonstrated that nitrogenase activity is specifically activated in situ by bacteria colonizing *RhiP* barley roots, but not in bacteria colonizing wild-type roots. Although this activity was suboptimal compared to the wild-type system, this work provides a proof-of-concept for the exclusive coupling of plant–microbe interactions in the field.

Results

Coexpression of *myo*-Inositol Uptake Genes Enhances SI Uptake and SI-Inducible Expression. Rhizopine perception in bacteria is dependent on activation of MocR, which drives expression from the rhizopine-inducible promoter P*mocB* in the presence of rhizopine (27). Initial tests of rhizopine perception in *Ac* carrying the first-generation rhizopine receiver plasmid pOPS0761 revealed that P*mocB*::*GFP* induction was poor, requiring 1 mM of SI to invoke a less than twofold induction (*SI Appendix*, Fig. S1). We reasoned that coexpression of a high-affinity rhizopine transporter might improve the sensitivity and dynamic range of rhizopine-inducible expression. Although the solute binding protein (SBP) MocB was encoded on our first-generation rhizopine-receiver plasmids, transmembrane components required for transport of rhizopine into the cytoplasm had not yet been identified. An ATP-binding cassette (ABC) transporter (IntABC) that accumulates the structurally related molecule *myo*-inositol is present in the model pea nodule symbiont *Rhizobium leguminosarum* bv. viceae 3841 (here termed *Rlv*) (36, 37). Given close homology of the *myo*-inositol SBP IntA with MocB, and the structural relatedness of their substrates (*SI Appendix*, Fig. S2), we explored whether the transmembrane components IntBC act in concert with MocB to transport SI. When *Rlv* carrying the rhizopine-receiver plasmid pOPS0046 was grown on *myo*-inositol to induce transcription of the native *intABC* genes, P*mocB*::*lux* expression was increased compared to bacteria grown on pyruvate at all concentrations of SI tested (*SI Appendix*, Fig S3*A*). We also compared P*mocB*::*lux* expression between a polar *intA*::mini-Tn*5* mutant of *Rlv* carrying pOPS0046 where *intABC* expression was abolished, against an identical strain additionally carrying plasmid pOPS0385, where *intBC* was constitutively expressed from the P*lac* promoter, and found that P*mocB*::*lux* expression was increased by *intBC* expression when 10 μM or more SI was supplemented into the growth media (*SI Appendix*, Fig. S3*B*). Thus, the *intBC* genes are required for a sensitive transcriptional response to SI.

To test whether coexpression of *intBC* would improve rhizopine-inducible expression in our model strain *Ac*, we assembled a "second-generation" rhizopine-receiver plasmid pSIR02 where *mocB-intBC* was expressed from the weak constitutive Anderson promoter P*J23115* (http://parts.igem.org/Promoters/Catalog/Anderson) and assembled the plasmid pSIR01 devoid of the *intBC* genes as a control (Fig. 1*A*). P*mocB*::*GFP* expression in *Ac* carrying pSIR02 was increased across all levels of SI-tested, with minimum induction achieved at 100 nM SI and maximum induction achieved with less than 10 μM SI supplemented into the growth media (Fig. 1*B*). In comparison, *Ac* carrying pSIR01 required 1 mM SI to elicit a less than twofold induction of P*mocB*::*GFP* (Fig. 1*B* and *SI Appendix*, Fig. S1*B*). The sensitivity of SI-perception by *Ac* carrying pSIR02 was therefore improved at least 10^3-fold. We also analyzed SI-inducible expression by flow-cytometry in the mCherry-labeled strain *Ac*Cherry carrying pSIR02 and found that ~36% (±SEM 0.3%) of cells exhibited GFP fluorescence above the mean 99th percentile of the noninduced cells (defined here as GFP^+) (Fig. 1*C* and Dataset S1). Lastly, we bio-assayed the intracellular contents of the *Ac* strains after 16-h incubation with 100 μM SI and found that cells carrying the pSIR02 plasmid harbored more SI relative to *Ac* carrying pSIR01 and wild-type *Ac* (Fig. 1*D* and Dataset S2). Overall, the data support IntBC functioning as transmembrane and ABC components, respectively, of a hybrid SI-uptake system utilizing MocB as the SBP.

Rhizopine Perception by *Ac* Colonizing *RhiP* Barley Roots. We previously developed a T1 rhizopine-producing (*RhiP*) barley line expressing codon optimized *R. leguminosarum idhA* and *Sinorhizobium meliloti* L5-30 *mosB* genes in multicopy under the control of *Zea mays* ubiquitin1 promoter and *Oryza sativa* ubiquitin1 promoter, respectively. Here, we generated a homozygous T2 *RhiP* line which, based on GC-MS analysis of metabolite extracts from 10-d-old seedlings ($n = 2$, 10 technical replicates

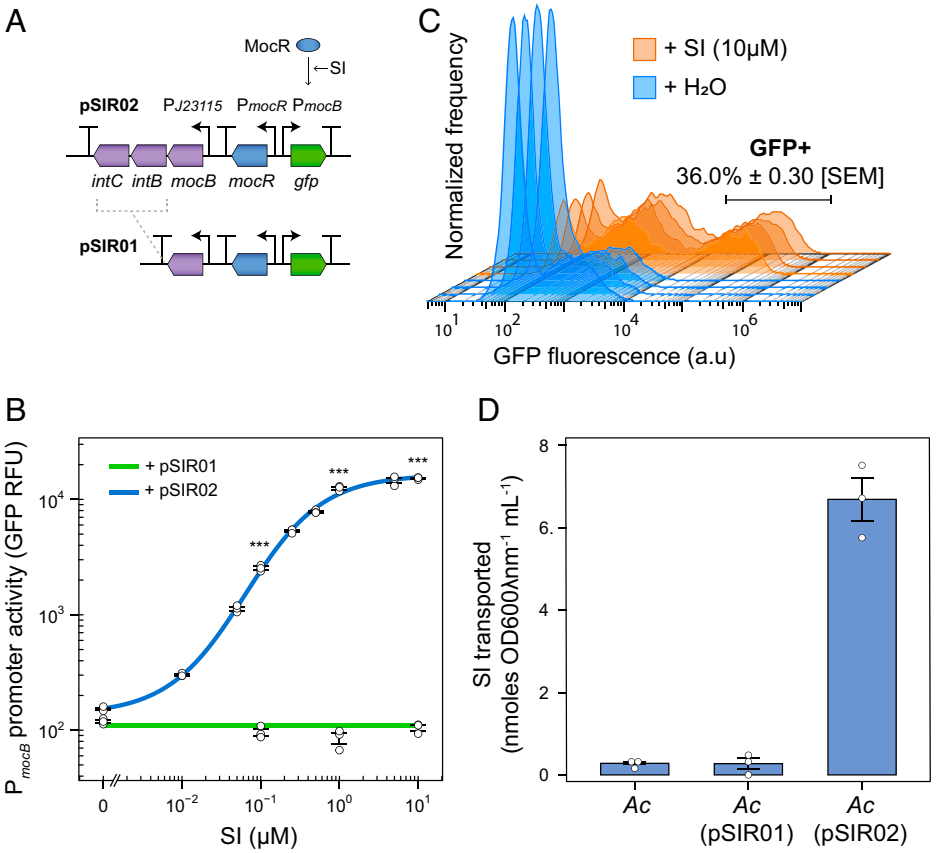

Fig. 1. Coexpression of the *myo*-inositol uptake genes *intBC* enhances rhizopine uptake and sensitivity of the transcriptional response. (*A*) Genetic schematics (not to scale) for the second-generation rhizopine receiver plasmid pSIR02 and a near identical plasmid lacking *intBC*. (*B*) P*mocB* promoter activity (RFU, defined as GFP fluorescence/ODλ600 nm) was measured in populations of *Ac* carrying pSIR01 or pSIR02. (*C*) Flow-cytometry analysis of *Ac*Cherry (pSIR02) cells induced with 10 μM SI or not induced after 18-h incubation ($n = 4$). Cells exhibiting GFP fluorescence above 20,000 a.u. were considered as GFP^+. Supplementary statistics supporting flow cytometry are provided in Dataset S1. (*D*) The intracellular contents of thrice washed *Ac* cells grown in the presence of 100 μM SI was bio-assayed for SI using *S. meliloti* carrying pOPS0046 and pOPS0385 as a sensor. Error bars represent one SEM ($n = 3$). Independent two-tailed Student's *t* tests were used to compare means. Exact values for $P > 0.05$ are given, $^{***}P < 0.001$.

each), produced 0.93 (±SEM 0.10) ng mg^{-1} root dry weight (Datasets S3 and S4), equating to approximately sevenfold less than the T1 *RhiP* line (27). To track rhizopine-inducible expression on the root surface, we inoculated plants with the constitutive mCherry-labeled strain *Ac*Cherry (pSIR02) and analyzed P*mocB*::*GFP* induction in single cells colonizing the root surface by confocal microscopy at 7 d postinoculation (dpi) (Fig. 2 *A* and *B* and *SI Appendix*, Fig. S4). GFP fluorescence above background levels was never observed in bacteria-colonizing wild-type plants, but was observed in a subpopulation of cells colonizing T2 *RhiP* barley, indicating P*mocB* was active.

*Ac*Cherry (pSIR02) cells were subsequently recovered from the rhizoplane and endosphere (here termed root-associated, RA) and from the rhizosphere (RS) of 9-dpi barley plants for quantification of SI-induction by flow-cytometry (38). Using the same experimental design, we also analyzed SI-induction by *Ac*Cherry (pSIR02) cells recovered from our previously reported T1 *RhiP* barley line. We found that 3.60% of cells isolated from the RA and 4.56% of cells isolated from the RS fraction of T2 *RhiP* plants exhibited GFP fluorescence higher than the mean 99th percentile of that detected in bacteria recovered from wild-type plants (here defined as GFP^+) (Fig. 2*C*), confirming these subpopulations were induced for P*mocB*::*GFP*. On T1 barley roots, 4.96% of cells isolated from the RA fraction and 10.70% of cells from the RS fraction were GFP^+, suggesting that the percentage of *Ac*Cherry (pSIR02) cells activated for *GFP* increases with increasing supply of rhizopine from the plant. Moreover, higher rhizopine production by the T1 *RhiP* barley translated to stronger induction of P*mocB*::*GFP* by *Ac*Cherry (pSIR02) cells (Fig. 2*D*).

We checked whether loss or silencing of the plasmid pSIR02 had occurred in bacterial populations recovered from wild-type and T2 *RhiP* barley roots. After regrowing bacteria recovered from three plants on nonselective universal minimal salts (UMS) agar, 60 of 60 ($n = 3$) of the colonies grew when patched onto UMS agar supplemented with kanamycin, indicating the plasmid pSIR02 was retained in all cases. Moreover, between 58% and 72% of colonies recovered from both fractions of the wild-type and T2 *RhiP* barley plants were induced for P*mocB*::*GFP* expression when regrown on UMS agar supplemented with 1 μM SI (*SI Appendix*, Fig. S5), indicating that the majority retained the capacity for functional rhizopine signaling.

In Vitro Rhizopine Control of N_2 Fixation. To establish rhizopine-dependent control of N_2 fixation in *Ac*, we used pSIR02 as a backbone to generate *nifA-rpoN* and $nifA_{L94Q/D95Q}$*rpoN* controller plasmids pSIN01 and pSIN02, respectively (Fig. 3*A*). These controllers were tested for functionality in the markerless *nifA* deletion mutant *Ac*Δ*nifA* grown under diazotrophic conditions (N-free liquid UMS with a starting atmosphere of 3% O_2 and ~97% N_2), by using a P*nifH*::*mCherry* reporter construct (pOPS1218) designed to monitor expression of the nitrogenase structural gene *nifH* and by performing acetylene reduction

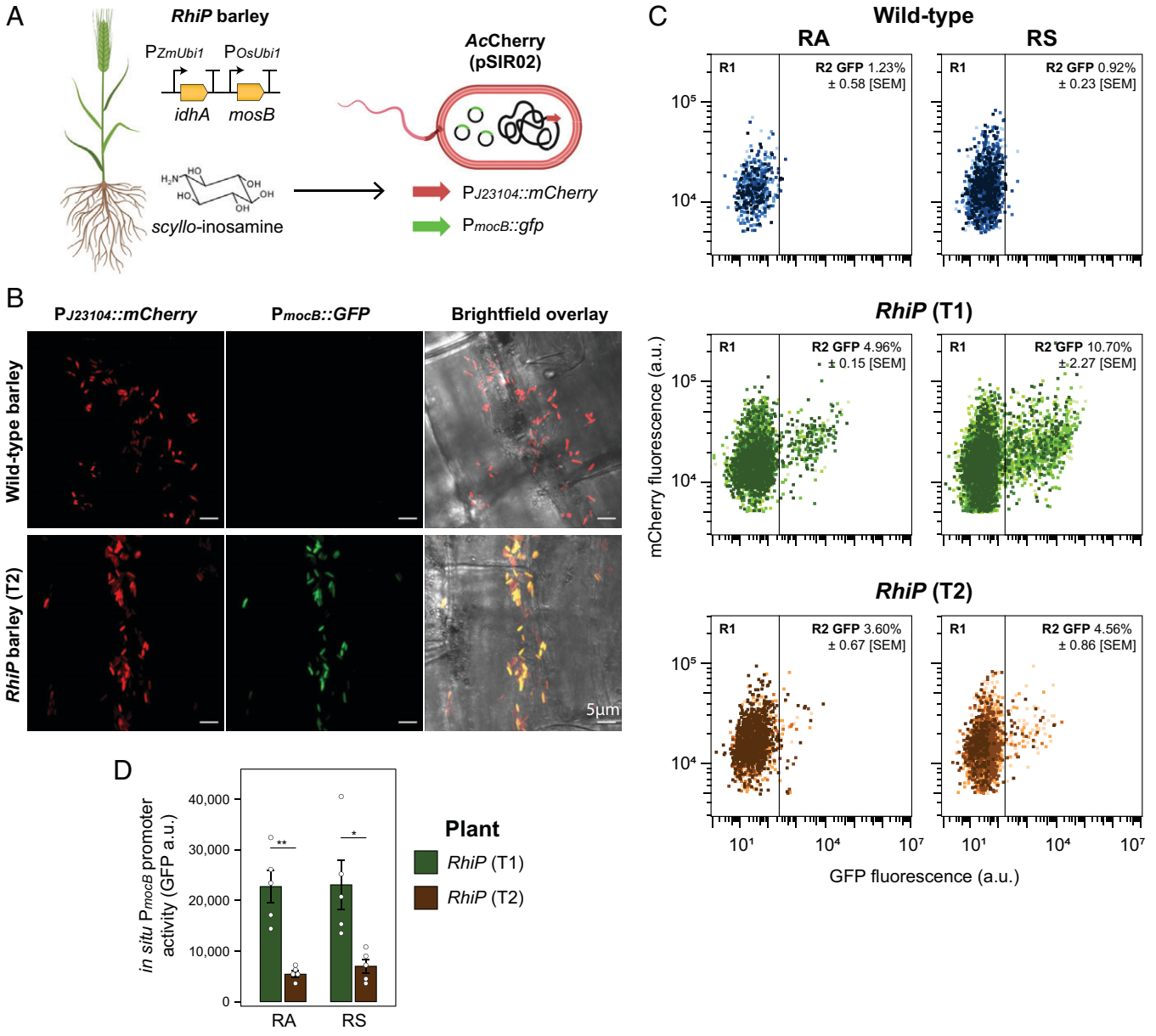

Fig. 2. Rhizopine-inducible expression on *RhiP* barley roots and in the rhizosphere. (*A*) Schematic representation of the experimental design to monitor P*mocB* expression on barley roots and in the rhizosphere. *Ac*Cherry cells are marked with a constitutively expressed mCherry gene allowing tracking. The strain additionally carries plasmid pSIR02. (*B*) Maximum-intensity projections showing mCherry and GFP fluorescence by *Ac*Cherry (pSIR02) cells colonizing the rhizoplane of wild-type and T2 *RhiP* barley at 9 dpi. Projections are representative of 15 images acquired from 3 whole lateral roots excised from 5 plants per treatment. (*C*) Flow-cytometry analysis of *Ac*Cherry (pSIR02) cells recovered from the rhizoplane and endosphere (RA) or rhizosphere (RS) of wild-type (blue), T1 *RhiP* (green), and T2 *RhiP* (brown) barley plants at 9 dpi ($n = 5$). Cells exhibiting mCherry fluorescence above 5,000 a.u. were analyzed. GFP$^+$ cells are defined as those exhibiting GFP fluorescence above the mean 99th percentile of the populations colonizing wild-type barley. Supplementary statistics supporting flow cytometry are provided in Dataset S5. (*D*) In situ P*mocB* promoter activity (median GFP fluorescence intensity) was measured for R2 GFP$^+$ bacteria in *C*. Error bars represent one SEM. Independent two-tailed Student's *t* tests were used to compare means. Exact values for $P > 0.05$ are given, $^*P < 0.05$, $^{**}P < 0.01$.

assays (ARAs) to assess nitrogenase activity. In *Ac*Δ*nifA* carrying pSIN01 or pSIN02 and pOPS1218, basal levels of P*nifH::mCherry* expression were detected in the absence of SI, while supplementation of 10 µM SI into the growth media resulted in above wild-type levels of P*nifH::mCherry* expression (Fig. 3*B*). No nitrogenase activity was detected for the same bacteria (devoid of pOPS1218) in the absence of SI, while supplementation of 10 µM SI into the growth media resulted in wild-type rates of nitrogenase activity, demonstrating tight binary control (Fig. 3*C*). As previously reported (15), induction of either *nifA-rpoN* or $nifA_{L94Q/D95Q}$-*rpoN* cassettes resulted in partial P*nifH* expression and nitrogenase activity in the presence of 10 mM NH_4Cl, with strains carrying $nifA_{L94Q/D95Q}$-*rpoN* exhibiting the highest partial activity at ∼50% that of wild-type strains grown in N-free conditions (Fig. 3).

In Situ Plant Host-Dependent Control of Associative N_2 Fixation. We next sought to demonstrate rhizopine control of *nifH* expression and nitrogenase activity by bacteria occupying the root systems of *RhiP* barley plants. Plasmid pSIN02 was modified by replacing the *GFP* gene downstream of P*mocB* with a divergently oriented P*nifH::GFP* reporter fusion (*SI Appendix*, Fig. S6) and the resulting plasmid pSIN03 was conjugated into *Ac*CherryΔ*nifA*. This strain was inoculated onto wild-type and

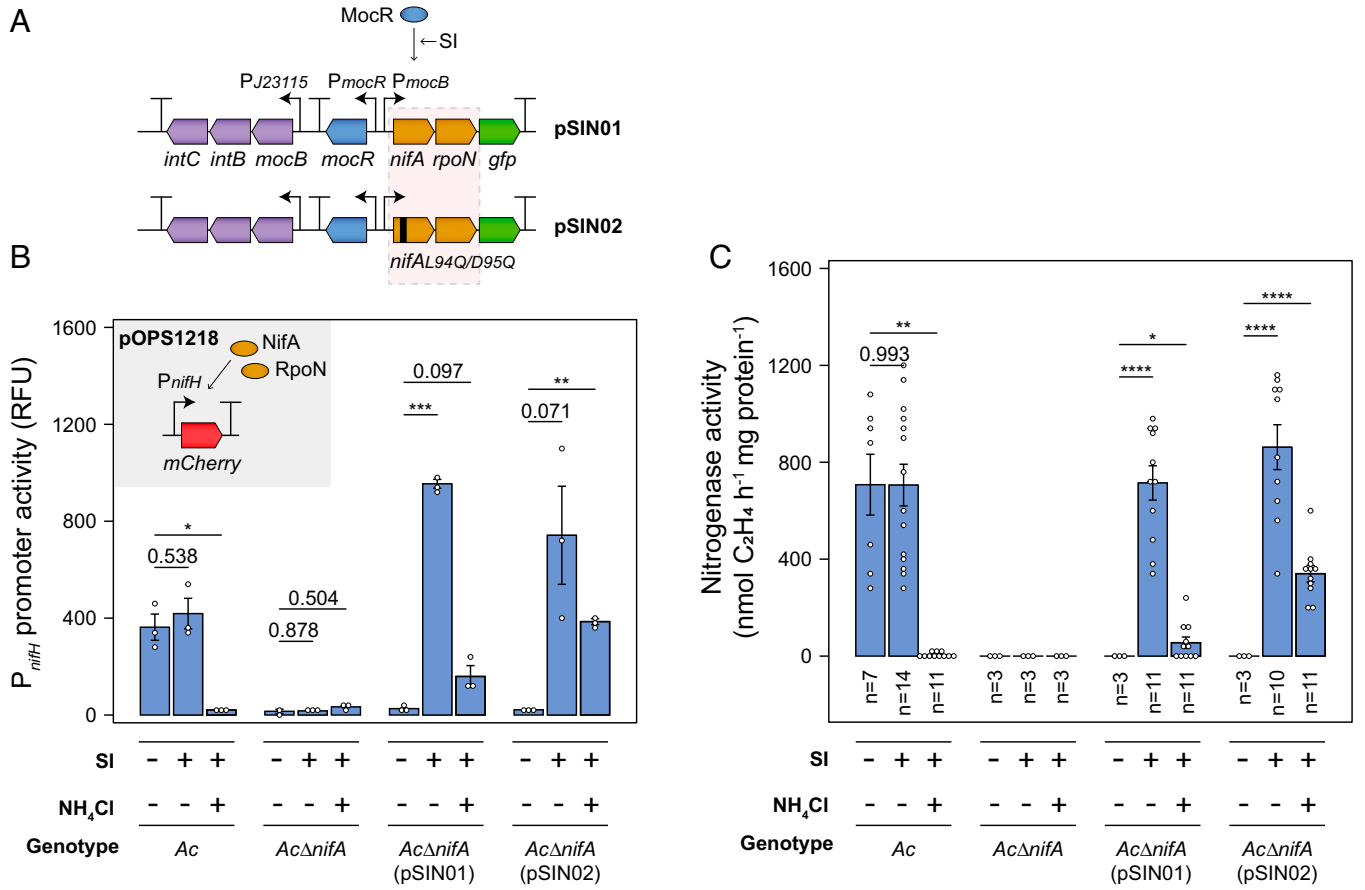

Fig. 3. In vitro rhizopine control of N_2-fixation. (*A*) Genetic schematics (not to scale) for *nifA-rpoN* and $nifA_{L94Q/D95Q}$ rhizopine controller plasmids. (*B*) P*nifH* promoter activity (RFU, defined as mCherry fluorescence/ODλ600 nm) was measured in populations of *Ac* and *Ac*ΔnifA ($n = 3$) carrying rhizopine controller plasmids and the reporter pOPS1218 grown in N_2-fixing conditions (N-free UMS supplemented with 20 mM succinate with a starting headspace of 3% O_2). SI and NH_4Cl was added to a final concentration of 10 μM and 10 mM, respectively, where indicated. (*C*) The same conditions were used to assess specific nitrogenase activity in *Ac* and *Ac*ΔnifA carrying rhizopine controller plasmids. Error bars represent one SEM ($n = 3$). Independent two-tailed Student's *t* tests were used to compare means. Exact values for $P > 0.05$ are given, $^*P < 0.05$, $^{**}P < 0.01$, $^{***}P < 0.001$, $^{****}P < 0.001$.

T2 *RhiP* barley and induction of P*nifH*::*GFP* in single cells on the root surface was assessed by confocal microscopy at 9 dpi after 24-h exposure to a headspace atmosphere of 1% O_2. As previously observed for SI-induction of P*mocB*::*GFP* on barley roots (Fig. 2 *A*–*C* and *SI Appendix*, Fig. S4), GFP fluorescence above background levels was never observed in bacteria colonizing wild-type plants, but was observed in a subpopulation of cells colonizing T2 *RhiP* barley (Fig. 4 *A* and *B* and *SI Appendix*, Fig. S7), indicating that *nifH* expression was induced. We also used flow-cytometry to quantify P*nifH*::*GFP* activation and found the results relatively mirrored those obtained for activation of P*mocB*::*GFP* (Fig. 2 *C* and *D*). On T1 barley roots, 22.92% and 22.32% of bacteria occupying the RA and RS fractions, respectively, were GFP^+, whereas on T2 barley roots 5.26% and 5.10% of bacteria occupying the RA and RS fractions, respectively, were GFP^+ (Fig. 4*C*). The mean GFP fluorescence was slightly higher in bacteria colonizing T1 *RhiP* barley compared to the T2 line, though this was not statistically significant (Fig. 4*D*).

To assess activation of N_2 fixation, in situ ARAs (38) were performed on wild-type and *RhiP* barley inoculated with *Ac*Δ*nifA* carrying pSIN02 at 9 dpi after adjusting the headspace of vessels to 1% O_2. Partially effective nitrogenase activity was induced on both T1 and T2 *RhiP* barley, whereas it was not detected on wild-type plants (Fig. 4*E*). Compared to the wild-type *Ac*, which produced ∼70 nmol C_2H_4 h^{-1} $plant^{-1}$ when colonizing wild-type or *RhiP* barley roots, nitrogenase in *Ac*Δ*nifA* carrying pSIN02 produced 10.24 nmols C_2H_4 h^{-1} $plant^{-1}$ when colonizing T1 *RhiP* barley roots and 3.63 nmols C_2H_4 h^{-1} $plant^{-1}$ when colonizing T2 *RhiP* barley roots, equating to ∼15% and 5% of wild-type levels, respectively. Importantly, the relative difference in nitrogenase activity detected for *Ac*Δ*nifA* carrying pSIN02 colonizing T1 *RhiP* plants compared to T2 *RhiP* plants was consistent with in situ P*mocB*::*GFP* (Fig. 2 *C* and *D*) and P*nifH* expression (Fig. 4 *C* and *D*) in the same plant lines, suggesting that in situ rhizopine-inducible nitrogenase activity is also dependent on the concentration of SI supplied by the plant. Upon recovering the bacteria and performing viable counts, it was apparent that root colonization by *Ac*Δ*nifA* bacteria carrying pSIN02 was mildly defective compared to *Ac* (*SI Appendix*, Fig. S8), which may partially contribute to the suboptimal nitrogenase activity observed in this strain. Nevertheless, the results reported here provide a proof-of-concept for the establishment of synthetic host-specific control over bacterial nitrogenase activity.

Discussion

In this work, we have stably engineered a homozygous rhizopine biosynthesis pathway into barley and concurrently improved rhizopine signaling circuitry in *Ac* to establish plant host-dependent control of *nifA-rpoN* cassettes driving expression and activity of

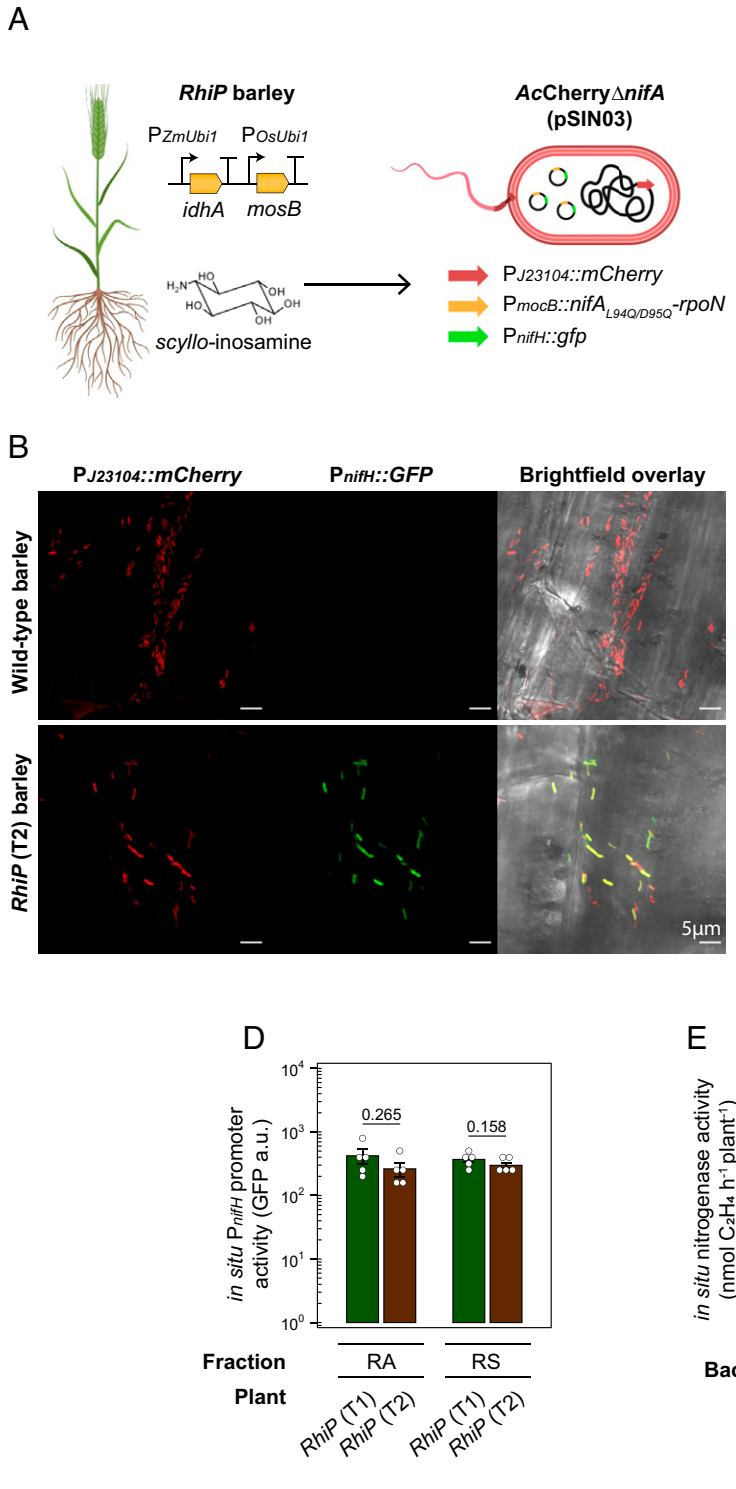

Fig. 4. In situ plant-dependent control of associative N_2-fixation (*A*) Schematic representation of the experimental design to monitor rhizopine-dependent P*nifH* expression on barley roots. *Ac*Cherry cells were marked with a constitutively expressed mCherry gene allowing tracking. The strain additionally carries plasmid pSIN03. (*B*) Maximum-intensity projections showing mCherry and GFP fluorescence by *Ac*CherryΔ*nifA* (pSIN03) cells colonizing the rhizoplane of wild-type and T2 *RhiP* barley at 9 dpi after 24-h exposure to 1% O_2 in the headspace. Projections are representative of 15 images acquired from 3 whole lateral roots excised from 5 plants per treatment. (*C*) Flow-cytometry analysis of *Ac*Cherry (pSIN03) cells recovered from the rhizopine and endosphere (RA) or rhizosphere (RS) of wild-type (blue), T1 *RhiP* (green), and T2 *RhiP* (brown) barley plants at 9 dpi after 24-h exposure to 1% O_2 in the headspace ($n = 5$). Cells exhibiting mCherry fluorescence above 1,500 a.u. were analyzed. GFP^+ cells are defined as those exhibiting GFP fluorescence above the mean 99th percentile of the populations colonizing wild-type barley. Supplementary statistics supporting flow-cytometry are provided in Dataset S7. (*D*) In situ P*nifH* promoter activity (median GFP fluorescence intensity) was measured for R2 GFP^+ bacteria in *C*. (*E*) In situ ARAs performed at 9 dpi after 48-h exposure to 1% O_2 in the headspace. Error bars represent one SEM. Independent two-tailed Student's *t* tests with Holm–Bonferroni adjusted *P* values were used to compare means. Exact values for $P > 0.05$ are given, $^{**}P < 0.01$.

nitrogenase. Despite the 10^3-fold improved sensitivity of in vitro rhizopine perception, our confocal microscopy and flow-cytometry experiments indicated that only a small fraction of the *Ac*Cherry (pSIR02) population occupying the *RhiP* barley roots responded to rhizopine signaling by expressing P*mocB::GFP* (Fig. 2). Likewise, in situ nitrogenase activity by *Ac*Δ*nifA* (pSIN02) colonizing *RhiP*

barley was suboptimal compared to wild-type *Ac* colonizing wild-type or *RhiP* barley (Fig. 4*E*). It seems unlikely that plasmid loss was responsible for these results given that all the *Ac*Cherry (pSIR02) colonies recovered from *RhiP* barley tested positive for kanamycin resistance conveyed by pSIR02. Silencing may have impeded efficient in situ rhizopine signaling and nitrogenase activity, although 58 to 72% of colonies recovered from T2 *RhiP* barley roots retained the capacity for SI induction of P*mocB::GFP* on agar plates (*SI Appendix*, Fig. S5). Finally, we found that *Ac*Δ*nifA* (pSIN02) are mildly defective in their ability to colonize barley roots, which may reduce nitrogenase activity per plant compared to the wild-type system. Our results overall suggested that increased rhizopine production by *RhiP* plants translated to stronger individual and population level SI perception and more effective nitrogenase expression and activity by bacteria (Figs. 2 and 4). Thus, further optimization of the rhizopine sensor and tuning of rhizopine biosynthesis gene expression may be necessary to generate a synthetic interaction that is better suited for practical use. It is crucial to note that excessive overexpression of SI biosynthesis genes would likely cause defects in plant metabolism that might influence biomass accumulation and increase the potential for enrichment of specialized bacteria capable of catabolizing the signal as a source of carbon or N in the field (28–30), as was previously reported for transgenic opine-producing plants (20–23). Thus, retaining SI biosynthesis at the minimum level required for a functional bacterial response will be crucial to optimize this circuitry.

Building on rhizopine control of N_2 fixation demonstrated here, our future aim is to engineer a more complete "synthetic symbiosis" where bacteria are also prompted to release fixed N to the host plant. This will require rewiring of nitrogen metabolism as *Ac* does not naturally release large quantities of fixed N into the growth media (39) but can be engineered to do so by deletion of the P_{II} genes *glnB* and *glnK* (40–42) or potentially by other strategies (18, 43–45). In addition, rhizopine signaling could be deployed by bacteria to initiate response signals to plants, establish biocontainment of bacteria in the root system, and develop relay signaling circuitry that will allow genetically incompatible bacteria to indirectly respond to rhizopine (9). Ultimately, we intend to utilize rhizopine signaling circuitry for control of bacterial traits within engineered barley nodules or "pseudo-nodules" where more fine-tuned signal and nutrient exchange would presumably exist (11, 12, 46). The biotechnological achievements made in this study represent a significant milestone toward the development of efficient partner-specific synthetic symbioses between cereals and bacteria.

Materials and Methods

Bacterial Strains and Growth Conditions. Bacterial strains used in this study are described in *SI Appendix*, Table S1. *Escherichia coli* was cultured on LB media and incubated at 37 °C, whereas *Rhizobium* and *Azorhizobium* strains were cultured on TY or UMS media and incubated at 28 °C or 37 °C, respectively. Where appropriate, UMS media was supplemented with 20 mM succinate or 30 mM pyruvate as a sole carbon source, 10 mM NH_4Cl as a sole nitrogen source, and 300 μM nicotinate (for *Ac* only). Antibiotics were added to media for *E. coli* and rhizobia, respectively, at the following concentrations: kanamycin 50, 100 μg mL^{-1}; gentamycin 10 μg mL^{-1}, 25 μg mL^{-1}; tetracycline 10 μg mL^{-1}, 5 μg mL^{-1}; carbenicillin 100 μg mL^{-1}; and spectinomycin 50 μg mL^{-1}. Strains harboring markerless *nifA* deletions were constructed via homologous recombination and sucrose counter selection (38) of plasmid pOPS1565 (*SI Appendix*, Table S2).

Plasmids. Plasmids were constructed using golden-gate assembly (47, 48), HiFi assembly (New England Biolabs), and yeast recombination (49), as described in *SI Appendix, Supplementary Materials and Methods*. All inserts were confirmed by Sanger sequencing. Plasmids were chemically transformed into *E. coli* strains (50) and mobilized into rhizobia via biparental conjugation with *E. coli* ST18 (51) or via triparental conjugation with a helper *E. coli* strain carrying plasmid pRK2013. Plasmids with R6K replicons were maintained at low copy number in *E. coli* EC100D Pir^+ where possible.

Reporter Assays. Single colonies were initially streaked onto 10 mL TY agar slopes in 28-mL universal vials and incubated for 2 to 3 d. Cells were washed from slopes in PBS, pelleted by centrifugation, and inoculated to an optical density (OD)λ600 nm of 0.1 into 96-deep-well culture plates, each well containing 500 μL UMS supplemented with the appropriate inducer. For P*nifH* induction assays, single colonies were initially streaked onto UMS agar slopes in 28-mL universal vials and incubated for 2 d prior to washing with PBS three times to remove residual nitrogen. Cells were finally resuspended in 5 mL N-free UMS liquid media with 20 mM succinate at ODλ600 nm 0.4 in 28-mL universal vials and the O_2 concentration was adjusted to 3% by flushing the headspace with N_2 gas for 1 h before sealing the vials with a rubber septum. Cultures were incubated for 18 h prior to 1:1 dilution with UMS and transfer into clear-bottom 96-well plates for quantification. Relative luminescence units (defined as RLU, luminescence/ODλ600 nm) were measured with a Promega GloMax multidetection system and relative fluorescence units (defined as RFU, mCherry/ODλ600 nm or GFP/ODλ600 nm) were measured with an Omega FLUOstar set at gain 1,000 for GFP and 1,500 for mCherry. GFP fluorescence was measured at excitation 485 nm and emission 520 nm, whereas mCherry fluorescence was measured at excitation 560 nm and emission 590 nm.

To bioassay intracellular SI in *Ac*, cells were washed from TY slopes after 2-d growth, pelleted by centrifugation, and inoculated at ODλ600 nm 0.4 into 28-mL universal vials containing 5 mL UMS supplemented with 100 μM SI. Cultures were incubated with vigorous shaking for 16 h, after which the culture ODλ600 nm was recorded, and 4 mL of cells were harvested by centrifugation. Cells were washed three-times in 5 mL PBS and resuspended in a final volume of 800 μL prior to mechanical lysis using a FastPrep-24 5G instrument. Cellular debris were removed by centrifugation and filter sterilization (0.22-μm pore size). Using *S. meliloti* 1021 carrying the SI receiver plasmid pOPS0046 (*PmocB::luxCDABE*) and plasmid pOPS0365 (*Plac::intBC*) as a biosensor, an SI standard curve was established and a four-parameter log-logistic model was fitted (Dataset S2) using the AAT Quest Graph Four Parameter Logistic (4PL) Curve Calculator (52, 53). SI was concurrently bio-assayed in 50-μL aliquots of the cleared intracellular lysates. Derived molar concentrations of SI in the total lysates were converted on a per cell basis using our experimentally derived conversion factor of ODλ600 nm $1.0 = 2 \times 10^8$ cells.

Engineering Rhizopine Biosynthesis in Barley. The rhizopine biosynthesis plasmid pEC12811 carried codon optimized *R. leguminosarum idhA* and *S. meliloti* L5-30 *mosB* genes expressed under the control of *Z. mays* ubiquitin1 promoter and *O. sativa* ubiquitin 1 promoter, respectively (27). The plasmid was integrated into the genome of Spring Golden Promise barley via *Agrobacterium*-mediated transformation (54) and plants were segregated to generate the homozygous T2 line *RhiP* (rhizopine-producing). Rhizopine production was confirmed in *RhiP* barley by metabolite extraction and GC-MS analysis of 10-d-old seedlings, as previously described (17). Raw data are provided in Datasets S3 and S4.

Confocal Microscopy. Barley plants for confocal microscopy were propagated in fire sand as previously described (38) and were inoculated with 2 mL of a thrice-washed N- and C-free UMS *Ac* cell suspension standardized to ODλ600 nm 0.1. To assess P*nifH* induction, the headspace atmosphere of 9-dpi barley plants was adjusted to 1% O_2 by flushing with N_2 gas for 1 h and the vessels were sealed with a rubber septum and returned to the growth chamber for a further 24 h prior to analysis. Dual-channel confocal images were taken of whole lateral roots of barley using a ZEISS LSM 880 Axio Imager 2 with a C-Apochromat 40×/1.2W Korr FCS M27 objective, as previously described (38). Excitation of GFP and mCherry was achieved using 488-nm (3% power) and 561-nm (4% power) lasers, respectively, and fluorescence emissions were collected using photomultiplier tube detectors for GFP (493 to 598 nm, gain 520

for *PmocB* or 580 for *PnifH* induction) and mCherry (detection 598 to 735, gain 640 for *PmocB* or 700 for *PnifH* induction). The *z*-stack images were captured in 0.5-μm slices with the pinhole set to 1.39 AU using LineSequential unidirectional scan mode. Maximum-intensity projections were created from *z*stacks using the Zen 3.2 Blue software and are representative of 15 projections imaged from 5 plants (3 per plant) for each treatment.

Flow Cytometry. For flow cytometry of bacteria grown in vitro, *Ac*Cherry (pSIR02) cells were induced with 10 μM SI as described above for reporter assays, diluted 1:100 in PBS, and analyzed using an Amnis Cellstream flow-cytometer equipped with an autosampler. GFP and mCherry was excited with 488- and 561-nm lasers, respectively. Singlets exhibiting mCherry fluorescence above 3,000 a.u. were considered as $mCherry^+$ bacteria for analysis. $mCherry^+$ bacteria exhibiting GFP fluorescence above the mean 99th percentile determined for noninduced cultures were considered as GFP^+ cells. The supplementary statistics for this analysis are provided (Dataset S1).

Barley plants for flow-cytometry experiments were propagated and inoculated as described for confocal microscopy experiments. After 9 dpi, bacteria occupying the RA and RS fractions were recovered and analyzed by flow-cytometry, as previously described (38). Singlets exhibiting mCherry fluorescence above the 5,000 a.u. or 1,500 a.u. were considered as $mCherry^+$ for analysis of P*mocB* and P*nifH* expression, respectively. $mCherry^+$ cells exhibiting GFP fluorescence above the mean 99th percentile determined for bacterial populations colonizing wild-type barley roots were defined as GFP^+. The supplementary statistics for these analyses are provided (Datasets S5 and S7).

Assessment of Plasmid Loss and Silencing in Bacteria Grown in Association with Barley Roots. To assess plasmid loss in *Ac*Cherry (pSIR02) cells recovered from the RS and RA fractions of *RhiP* barley from flow-cytometry experiments, cell suspensions were plated on nonselective UMS agar and incubated 2 d. Sixty colonies recovered from each fraction of three *RhiP* plants were patched onto UMS agar supplemented with kanamycin, and onto nonselective UMS agar as a control. As the kanamycin resistance gene was expressed from pSIR02, resistant colonies were scored as having retained the plasmid. Silencing of pSIR02 was also assessed in the RS and RA fractions recovered from three wild-type and *RhiP* barley plants by plating cell suspensions on UMS agar supplemented with kanamycin or the same media additionally containing 1 μM SI. Plates were imaged using a Leica M165 FC fluorescent stereo microscope fitted with a CLS100x cold light source and DFC310 FX. To assess GFP induction, dual-channel images captured using dsRed and GFP filters were converted to 8-bit using ImageJ (55). $mCherry^+$ colonies were demarcated for analysis in the dsRed channel using the thresholding tool (gray value > 20 and area > 100 $pixel^2$) and these coordinates were superimposed over the GFP channel images. Colonies were scored as GFP^+ if the maximum gray value exceeded 25. At least 32 colonies were analyzed per biological replicate. The raw data are provided (Dataset S6).

ARAs. For ARAs of free-living bacteria in liquid cultures, cells were prepared and inoculated at ODλ600 nm 0.4 into 5 mL N-free UMS media supplemented with 20 mM succinate in 28-mL universal vials as described for P*nifH* induction assays. The starting headspace atmosphere was adjusted to 3% O_2 by placing the vials on a rotary shaker in a controlled atmosphere of 97% N_2 for 1 h. To initiate the assay, 10% of the total headspace atmosphere was replaced with C_2H_2 using a 20-mL syringe and needle and the cultures were incubated at 37 °C for 10 h or 24 h prior measuring the production of C_2H_4 using a PerkinElmer, Clarus 480 gas chromatograph equipped with a HayeSep N (80 to 100 MESH) 584 column. A second measurement was taken 2 h later and the rate of nitrogenase activity between these time points was calculated as previously described (38). Subsequently, 2 mL of the bacterial culture was harvested by centrifugation, washed in PBS, and mechanically lysed using a FastPrep-24 5G instrument. BCA assays were used to determine total protein content and specific nitrogenase activity calculated. In situ ARAs of bacteria inoculated onto barley plants were performed after 9 dpi with a headspace atmosphere of 1% O_2 and 10% C_2H_4 as previously described (38).

Statistical Analyses. Statistical analyses were carried out using the R package Rstatix (56). Dose–response curves were fitted using the R package drc (53). Details of each statistical analysis are outlined in the figure captions.

Data Availability. All study data are included in the main text and supporting information. All research materials supporting this publication can be accessed by contacting corresponding authors T.L.H. or P.S.P.

ACKNOWLEDGMENTS. This work was supported by the Biotechnology and Biological Sciences Research Council (BB/T006722/1, BB/T001801/1, and BB/M011224/1), the Gatsby Foundation (GAT3395/GLH) and by the NSF (NSF-1331098). T.L.H. is the recipient of an 1851 Royal Commission for the Exhibition of 1851 Research Fellowship (RF-2019-100238) and Wolfson College, University of Oxford Junior Research Fellowship.

Author affiliations: [a]Department of Plant Sciences, University of Oxford, Oxford OX1 3RB, United Kingdom; [b]Sainsbury Laboratory, University of Cambridge, Cambridge CB2 1LR, United Kingdom; [c]Department of Microbiological Sciences, North Dakota State University, Fargo, ND 58105; [d]Synthetic Biology Center, Department of Biological Engineering, Massachusetts Institute of Technology, Cambridge, MA 02139; and [e]Biochemistry and Metabolism, The John Innes Centre, Norwich NR4 7UH, United Kingdom

1. M. S. Santos, M. A. Nogueira, M. Hungria, Microbial inoculants: Reviewing the past, discussing the present and previewing an outstanding future for the use of beneficial bacteria in agriculture. *AMB Express* **9**, 205–205 (2019).
2. G. W. O'Hara, The role of nitrogen fixation in crop production. *J. Crop Prod.* **1**, 115–138 (1998).
3. M. Rosenblueth *et al.*, Nitrogen fixation in cereals. *Front. Microbiol.* **9**, 1794 (2018).
4. D. F. Herridge, M. B. Peoples, R. M. Boddey, Global inputs of biological nitrogen fixation in agricultural systems. *Plant Soil* **311**, 1–18 (2008).
5. S. L. Kandel, P. M. Joubert, S. L. Doty, Bacterial endophyte colonization and distribution within plants. *Microorganisms* **5**, 77 (2017).
6. H. E. Knights, B. Jorrin, T. L. Haskett, P. S. Poole, Deciphering bacterial mechanisms of root colonization. *Environ. Microbiol. Rep.* **13**, 428–444 (2021).
7. M. Díaz-Zorita, M. V. Fernández-Canigia, Field performance of a liquid formulation of *Azospirillum brasilense* on dryland wheat productivity. *Eur. J. Soil Biol.* **45**, 3–11 (2009).
8. S. Dobbelaere *et al.*, Responses of agronomically important crops to inoculation with *Azospirillum*. *Funct. Plant Biol.* **28**, 871–879 (2001).
9. T. L. Haskett, A. Tkacz, P. S. Poole, Engineering rhizobacteria for sustainable agriculture. *ISME J.* **15**, 949–964 (2021).
10. M. Bueno Batista, R. Dixon, Manipulating nitrogen regulation in diazotrophic bacteria for agronomic benefit. *Biochem. Soc. Trans.* **47**, 603–614 (2019).
11. C. Rogers, G. E. Oldroyd, Synthetic biology approaches to engineering the nitrogen symbiosis in cereals. *J. Exp. Bot.* **65**, 1939–1946 (2014).
12. G. E. D. Oldroyd, R. Dixon, Biotechnological solutions to the nitrogen problem. *Curr. Opin. Biotechnol.* **26**, 19–24 (2014).
13. S. Burén, G. López-Torrejón, L. M. Rubio, Extreme bioengineering to meet the nitrogen challenge. *Proc. Natl. Acad. Sci. U.S.A.* **115**, 8849–8851 (2018).
14. L. Curatti, L. M. Rubio, Challenges to develop nitrogen-fixing cereals by direct *nif*-gene transfer. *Plant Sci.* **225**, 130–137 (2014).
15. M. H. Ryu *et al.*, Control of nitrogen fixation in bacteria that associate with cereals. *Nat. Microbiol.* **5**, 314–330 (2020).
16. B. A. Geddes *et al.*, Use of plant colonizing bacteria as chassis for transfer of N_2-fixation to cereals. *Curr. Opin. Biotechnol.* **32**, 216–222 (2015).
17. S. E. Bloch, M.-H. Ryu, B. Ozaydin, R. Broglie, Harnessing atmospheric nitrogen for cereal crop production. *Curr. Opin. Biotechnol.* **62**, 181–188 (2020).
18. R. Colnaghi, A. Green, L. He, P. Rudnick, C. Kennedy, Strategies for increased ammonium production in free-living or plant associated nitrogen fixing bacteria. *Plant Soil* **194**, 145–154 (1997).
19. R. G. Fray *et al.*, Plants genetically modified to produce N-acylhomoserine lactones communicate with bacteria. *Nat. Biotechnol.* **17**, 1017–1020 (1999).
20. M. A. Savka, S. K. Farrand, Modification of rhizobacterial populations by engineering bacterium utilization of a novel plant-produced resource. *Nat. Biotechnol.* **15**, 363–368 (1997).
21. H. Mansouri, A. Petit, P. Oger, Y. Dessaux, Engineered rhizosphere: The trophic bias generated by opine-producing plants is independent of the opine type, the soil origin, and the plant species. *Appl. Environ. Microbiol.* **68**, 2562–2566 (2002).
22. P. Oger, A. Petit, Y. Dessaux, Genetically engineered plants producing opines alter their biological environment. *Nat. Biotechnol.* **15**, 369–372 (1997).
23. S. Mondy *et al.*, An increasing opine carbon bias in artificial exudation systems and genetically modified plant rhizospheres leads to an increasing reshaping of bacterial populations. *Mol. Ecol.* **23**, 4846–4861 (2014).
24. S. Wellington, E. P. Greenberg, Quorum sensing signal selectivity and the potential for interspecies cross talk. *MBio* **10**, e00146–e00119 (2019).
25. Y. Dessaux, E. Chapelle, D. Faure, "Quorum sensing and quorum quenching in soil ecosystems" in *Biocommunication in Soil Microorganisms*, G. Witzany, Ed. (Springer, Berlin, Heidelberg, 2011), pp. 339–367.
26. C. S. Nautiyal, P. Dion, Characterization of the opine-utilizing microflora associated with samples of soil and plants. *Appl. Environ. Microbiol.* **56**, 2576–2579 (1990).
27. B. A. Geddes *et al.*, Engineering transkingdom signalling in plants to control gene expression in rhizosphere bacteria. *Nat. Commun.* **10**, 3430 (2019).
28. P. J. Murphy, W. Wexler, W. Grzemski, J. P. Rao, D. Gordon, Rhizopines–Their role in symbiosis and competition. *Soil Biol. Biochem.* **27**, 525–529 (1995).
29. D. M. Gordon, M. H. Ryder, K. Heinrich, P. J. Murphy, An experimental test of the rhizopine concept in *Rhizobium meliloti*. *Appl. Environ. Microbiol.* **62**, 3991–3996 (1996).

30. M. Wexler, D. Gordon, P. J. Murphy, The distribution of inositol rhizopine genes in *Rhizobium* populations. *Soil Biol. Biochem.* **27**, 531–537 (1995).
31. P. J. Murphy *et al.*, Genes for the catabolism and synthesis of an opine-like compound in *Rhizobium meliloti* are closely linked and on the Sym plasmid. *Proc. Natl. Acad. Sci. U.S.A.* **84**, 493–497 (1987).
32. S. Subramoni, N. Nathoo, E. Klimov, Z.-C. Yuan, *Agrobacterium* tumefaciens responses to plant-derived signaling molecules. *Front Plant Sci* **5**, 322 (2014).
33. J. Oetjen, B. Reinhold-Hurek, Characterization of the DraT/DraG system for posttranslational regulation of nitrogenase in the endophytic betaproteobacterium *Azoarcus* sp. strain BH72. *J. Bacteriol.* **191**, 3726–3735 (2009).
34. Y. Zhang, R. H. Burris, P. W. Ludden, G. P. Roberts, Presence of a second mechanism for the posttranslational regulation of nitrogenase activity in *Azospirillum brasilense* in response to ammonium. *J. Bacteriol.* **178**, 2948–2953 (1996).
35. K.-B. Lee *et al.*, The genome of the versatile nitrogen fixer *Azorhizobium caulinodans* ORS571. *BMC Genomics* **9**, 271 (2008).
36. J. Fry, M. Wood, P. S. Poole, Investigation of myo-inositol catabolism in *Rhizobium leguminosarum* bv. viciae and its effect on nodulation competitiveness. *Mol. Plant Microbe Interact.* **14**, 1016–1025 (2001).
37. R. Karunakaran *et al.*, Transcriptomic analysis of *Rhizobium leguminosarum* biovar viciae in symbiosis with host plants *Pisum sativum* and *Vicia cracca*. *J. Bacteriol.* **191**, 4002–4014 (2009).
38. T. L. Haskett, H. E. Knights, B. Jorrin, M. D. Mendes, P. S. Poole, A simple in situ assay to assess plant-associative bacterial nitrogenase activity. *Front. Microbiol.* **12**, 690439 (2021).
39. M. M. A. Ferdinandy-van Vlerken, E. Jeronimus, K. Maarsen, A. H. Stouthamer, H. W. van Verseveld, Absence of ammonia excretion during free-living, nitrogen-fixing growth of *Azorhizobium caulinodans*. *FEMS Microbiol. Lett.* **79**, 45–49 (1991).
40. N. Michel-Reydellet, N. Desnoues, M. de Zamaroczy, C. Elmerich, P. A. Kaminski, Characterisation of the *glnK-amtB* operon and the involvement of AmtB in methylammonium uptake in *Azorhizobium caulinodans*. *Mol. Gen. Genet.* **258**, 671–677 (1998).
41. N. Michel-Reydellet, P. A. Kaminski, *Azorhizobium caulinodans* P_{II} and GlnK proteins control nitrogen fixation and ammonia assimilation. *J. Bacteriol.* **181**, 2655–2658 (1999).
42. N. Michel-Reydellet, N. Desnoues, C. Elmerich, P. A. Kaminski, Characterization of *Azorhizobium caulinodans glnB* and *glnA* genes: Involvement of the $P(_{II})$ protein in symbiotic nitrogen fixation. *J. Bacteriol.* **179**, 3580–3587 (1997).
43. T. Schnabel, E. Sattely, Engineering posttranslational regulation of glutamine synthetase for controllable ammonia production in the plant symbiont *Azospirillum brasilense*. *Appl. Environ. Microbiol.* **87**, e0058221 (2021).
44. I. Martinez-Argudo, R. Little, R. Dixon, Role of the amino-terminal GAF domain of the NifA activator in controlling the response to the antiactivator protein NifL. *Mol. Microbiol.* **52**, 1731–1744 (2004).
45. M. Bueno Batista, P. Brett, C. Appia-Ayme, Y.-P. Wang, R. Dixon, Disrupting hierarchical control of nitrogen fixation enables carbon-dependent regulation of ammonia excretion in soil diazotrophs. *PLoS Genet.* **17**, e1009617 (2021).
46. K. Schiessl *et al.*, NODULE INCEPTION recruits the lateral root developmental program for symbiotic nodule organogenesis in *Medicago truncatula*. *Curr. Biol.* **29**, 3657–3668.e5 (2019).
47. B. A. Geddes, M. A. Mendoza-Suárez, P. S. Poole, A bacterial expression vector archive (BEVA) for flexible modular assembly of golden gate-compatible vectors. *Front. Microbiol.* **9**, 3345 (2019).
48. E. Weber, C. Engler, R. Gruetzner, S. Werner, S. Marillonnet, A modular cloning system for standardized assembly of multigene constructs. *PLoS One* **6**, e16765 (2011).
49. R. M. Shanks, N. C. Caiazza, S. M. Hinsa, C. M. Toutain, G. A. O'Toole, *Saccharomyces cerevisiae*-based molecular tool kit for manipulation of genes from gram-negative bacteria. *Appl. Environ. Microbiol.* **72**, 5027–5036 (2006).
50. H. Inoue, H. Nojima, H. Okayama, High efficiency transformation of *Escherichia coli* with plasmids. *Gene* **96**, 23–28 (1990).
51. S. Thoma, M. Schobert, An improved *Escherichia coli* donor strain for diparental mating. *FEMS Microbiol. Lett.* **294**, 127–132 (2009).
52. AAT Bioquest, Quest Graph Four Parameter Logistic (4PL) Curve Calculator. (2021). https://www.aatbio.com/tools/four-parameter-logistic-4pl-curve-regression-online-calculator. Accessed 21 December 2021.
53. C. Ritz, F. Baty, J. C. Streibig, D. Gerhard, Dose-response analysis using R. *PLoS One* **10**, e0146021 (2015).
54. W. A. Harwood, A protocol for high-throughput *Agrobacterium*-mediated barley transformation. *Methods Mol. Biol.* **1099**, 251–260 (2014).
55. C. A. Schneider, W. S. Rasband, K. W. Eliceiri, NIH Image to ImageJ: 25 years of image analysis. *Nat. Methods* **9**, 671–675 (2012).
56. R. C. Team, *R: A language and environment for statistical computing*. (R Foundation for Statistical Computing. Vienna, Austria, 2021). http://www.R-project.org/.